

KAWASAKI STEEL TECHNICAL REPORT

No.3 (September 1981)

Earthquake Response Analysis of No.6 Blast Furnace of Chiba Works

Masahiro Ishida, Michihiko Hara, Satoru Nishiyama, Ikuo Jo

Synopsis :

Earthquake measurements have been taken since 1977 in order to investigate the dynamic behavior of No.6 blast furnace and its surrounding soft ground at Chiba Works. Two severe earthquakes of the so-called "directly under" type, hit the Kanto districts on September 24 and 25, 1980, registering Richter magnitudes of 6.0 and 6.1, respectively. Their epicenters were located near Chiba Works, and maximum response acceleration at the super-and sub-structures of No.6 blast furnace and its surrounding soft ground is the largest of all the earthquakes ever observed. In this report, the results of earthquake observations are discussed in comparison with those of theoretical approaches, namely, analytical simulations using lumped mass idealization. The following conclusions may be drawn from the observation and analysis of actual earthquakes. (1) Judging from the response spectrum, the structure is more liable to resonate with the so-called "longdistance" type earthquake than with the "directly under" type, and yet in the latter type earthquake, the structure is strongly affected by the vertical motion of the earthquake. Further study in this aspect is required to be expedited. (2) Story-shearing coefficients at the sub-structure calculated from response acceleration of actual earthquakes approximate to the design values, but those at the super-structure exceed them. (3) It is predicted that if earthquakes occur that have substratum acceleration a little less than eleven times that in the biggest "directly under" type earthquake (June 12, 1978), or twice that in the biggest "long-distance" type (Sept. 24, 1980), the story shear coefficient at the top story will exceed the design value.

(c)JFE Steel Corporation, 2003

The body can be viewed from the next page.

Earthquake Response Analysis of No. 6 Blast Furnace of Chiba Works*

Masahiro ISHIDA** Michihiko HARA** Satoru NISHIYAMA***
Ikuo Jo**

Earthquake measurements have been taken since 1977 in order to investigate the dynamic behavior of No. 6 blast furnace and its surrounding soft ground at Chiba Works.

Two severe earthquakes of the so-called "directly under" type, hit the Kanto districts on September 24 and 25, 1980, registering Richter magnitudes of 6.0 and 6.1, respectively. Their epicenters were located near Chiba Works, and maximum response acceleration at the super-and sub-structures of No. 6 blast furnace and its surrounding soft ground is the largest of all the earthquakes ever observed.

In this report, the results of earthquake observations are discussed in comparison with those of theoretical approaches, namely, analytical simulations using lumped mass idealization.

The following conclusions may be drawn from the observation and analysis of actual earthquakes.

- (1) *Judging from the response spectrum, the structure is more liable to resonate with the so-called "longdistance" type earthquake than with the "directly under" type, and yet in the latter type earthquake, the structure is strongly affected by the vertical motion of the earthquake. Further study in this aspect is required to be expedited.*
- (2) *Story-shearing coefficients at the sub-structure calculated from response acceleration of actual earthquakes approximate to the design values, but those at the super-structure exceed them.*
- (3) *It is predicted that if earthquakes occur that have substratum acceleration a little less than eleven times that in the biggest "directly under" type earthquake (June 12, 1978), or twice that in the biggest "long-distance" type (Sept. 24, 1980), the story shear coefficient at the top story will exceed the design value.*

1 Introduction

After an earthquake on the early morning of September 24, 1980, the Tokyo metropolitan area was hit again before dawn of the 25th by the so-called "directly under" type earthquake of magnitude 6 on the Richter scale. The mechanism of earthquake occurrence in the Kanto district is classified into two categories: ① gigantic earthquakes in the Sagami trough, and ② "directly under" type earthquakes that occur in shallow ground in and around Tokyo. The "directly under" type earthquakes include two types; a type that occurs due to creeping-in of a plate,

and the other caused by the destruction of active faults. The latter is deemed the more probable cause of the recent earthquakes and it is highly possible that seismic activities in the area called a "nest of earthquakes" have started recurring.

This report clarifies the characteristics of heavy foundations, such as the blast furnace foundation, viewed from the standpoint of aseismic engineering, on the basis of the earthquake response record obtained by seismic observation conducted at No. 6 BF of Chiba Works and its surrounding soft ground, and makes this study a reference material for future seismic designs.

2 Sites of Seismic Observation and Analysis Flow

In the earthquake response analysis, the strong earthquake motion of EL CENTRO earthquake, etc.,

* Originally published in *Kawasaki Steel Giho*, 13(1981) 2, pp. 97-108

** Engineering Division

*** Chiba Works

observed on the ground is used as the input earthquake wave after converting it into the bed rock wave by the theory of the multiple reflections. However, this is, after all, only a second-best measure for the aseismic design. The best way is to input the waveform obtained directly by seismic observation. With the intention of measuring the dynamic deformation characteristics of soft layers around No. 6 BF of Chiba Works, piezo-electric type accelerometers were installed at 4 different depths, i.e., ground surface (depth 0.4 m), 8 m, 25 m and 50 m deep. Further, a total of 14 servotype accelerometers were installed on the foundation of No. 6 BF and on its superstructure. Their locations are shown in Fig. 1.

Fig. 2 shows an outline of the seismic observation arrangement. The measurement system is shown on the left side of the figure and the analysis flow chart after recovery of data on the right side.

Signals are sent constantly from each seismograph to the data recorder through the amplifier and time delay unit, and the signals are sent to the automatic starter simultaneously. When the automatic starter detects velocity or acceleration greater than the set value due to earthquakes, the starter activates the data recorder to print the time of starting. The time delay unit of delay time 3 sec. is inserted to prevent missing of the record of initial part of earthquake. The seismic record collected on the magnetic tape as analog data through the above-mentioned route is stored on the magnetic tape or disc unit after being converted into numerical data, and used as basic data for various analyses.

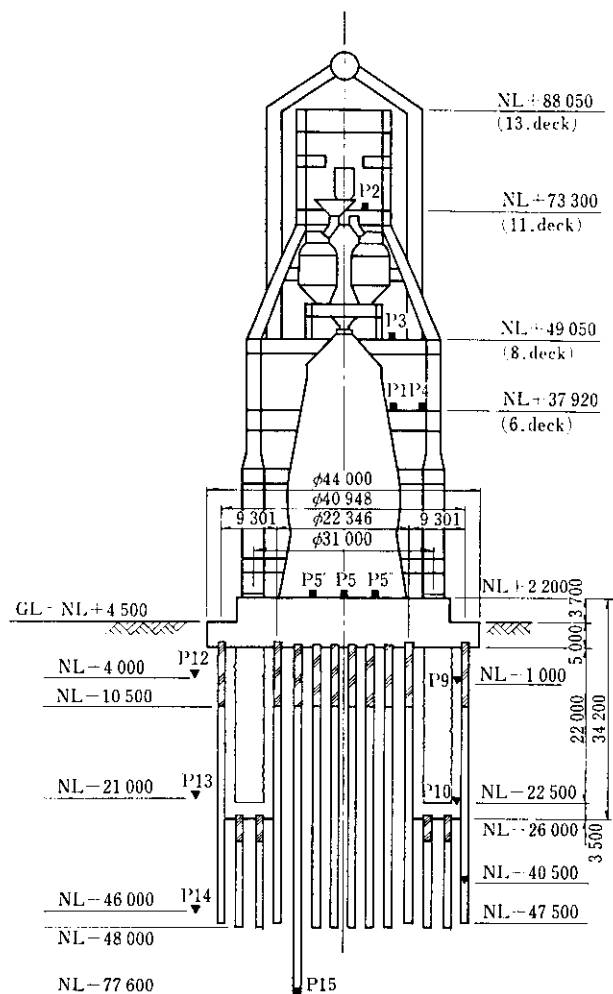


Fig. 1 Location of seismometers at No. 6 blast furnace of Chiba Works

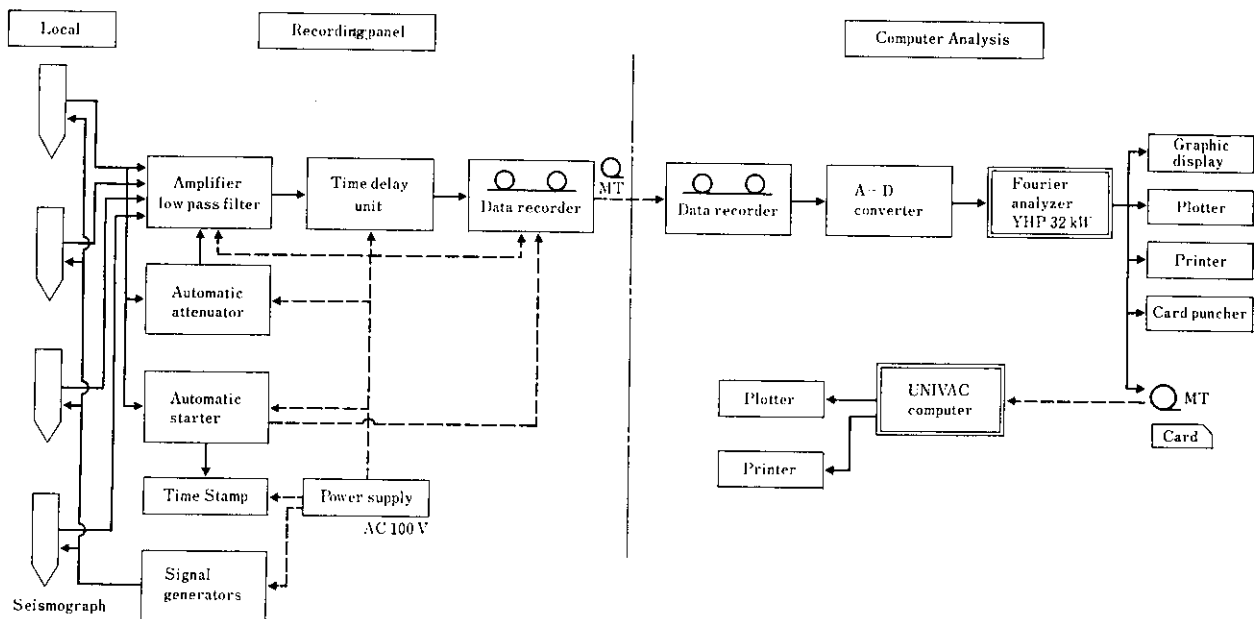


Fig. 2 Earthquake measurement system and analysis flow chart

Table 1 List of observed earthquakes

Date	June 12, 1978	Sept.24, 1980	Sept.25, 1980
Time	17 : 14	04 : 10	02 : 54
Hypocenter Location	Off Miyagi Pref.	South-western part of Ibaragei Pref.	Central part of Chiba Pref.
Latitude	38°09'	36°06'	35°30'
Longitude	142°10'	139°42'	140°12'
Depth	40 km	60 km	70 km
Magnitude	7.4	6.0	6.1
Epicentral distance	345 km	70.2 km	18.7 km
Seismic intensity	IV	III	IV

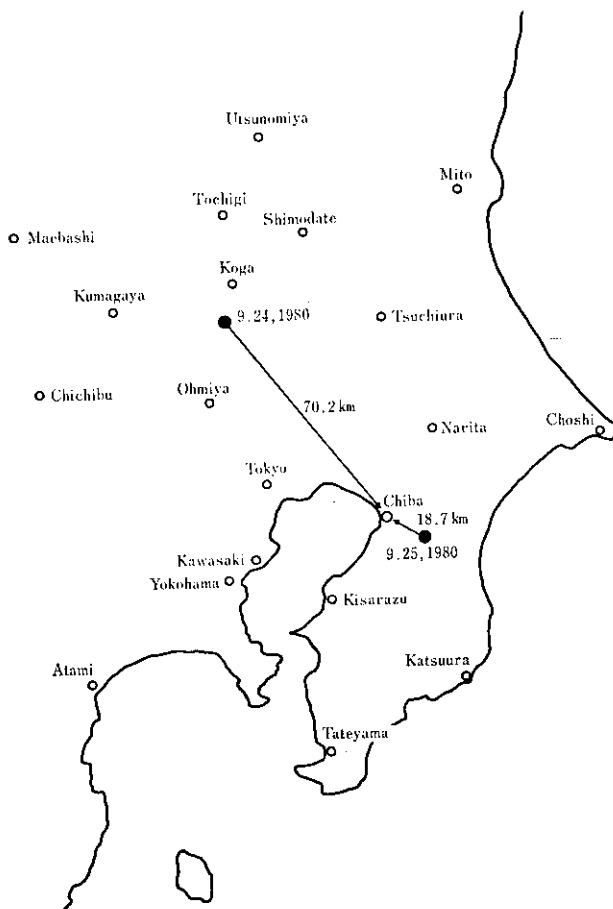


Fig. 3 Hypocenter location

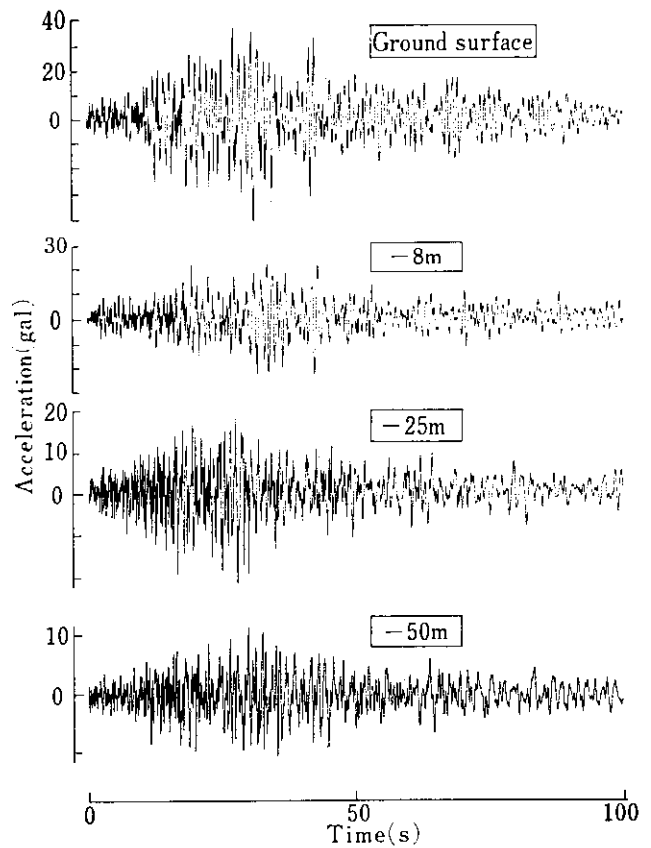


Fig. 4 Acceleration records (June 12, 1978)

3 Results of Seismic Observation

Table 1 shows an outline of the “directly under” type earthquakes which occurred on September 24 and 25, 1980. In the case of the earthquake on the 25th, 4 aftershocks took place intermittently within two hours after the main shock which occurred at 2:54. Their description is omitted here. The table also includes an outline of long-distance type earthquake which occurred on June 12, 1978.

The hypocenter locations of recent earthquakes are shown in Fig. 3. The hypocenter shifted from Ibaraki Prefecture (24th) to Chiba Prefecture (25th), and Chiba Works is located on a straight line connecting the two hypocenter locations. Though this may be an accidental phenomenon, precautions are necessary.

Figs. 4 and 5 show examples of acceleration records observed this time. The maximum acceleration of ground is summarized in Table 2. The table includes the maximum acceleration of the offshore Miyagi Prefecture earthquake which occurred on June 12, 1978. Fig. 6 shows vertical distributions of the maximum acceleration in the ground corresponding to Table 2. The left side of the figure shows the vertical

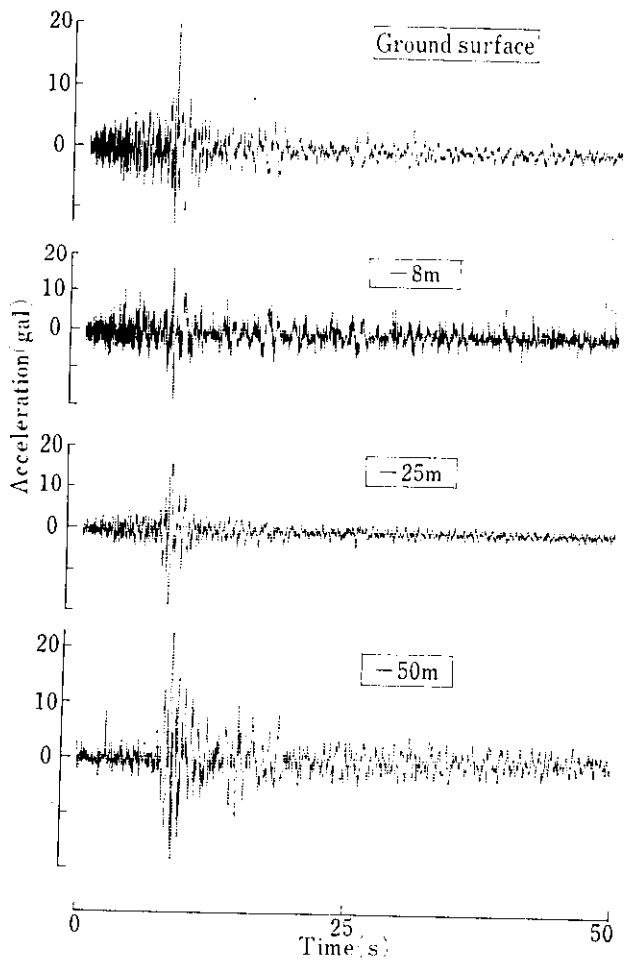


Fig. 5 Acceleration records (Sept. 25, 1980)

distribution of maximum acceleration at the offshore Miyagi Prefecture earthquake which was of a long-distance type, and the right side shows that of the central Chiba Prefecture earthquake which was of a "directly under" type. According to the announcement made by the Meteorological Agency, seismic intensity of the two earthquakes in Chiba Prefecture was IV. However, a considerable difference is observed between the two types of vertical distribution of the

Table 2 Maximum acceleration of observed earthquakes (Ground)

Location	Component	Response Max. Acc. (gal)	
		June 12, 1978	Sept. 25, 1980
Ground surface	H_{x-x}	41.5	20.0
	H_{y-y}	28.0	19.0
	Z	16.0	21.0
-8 m	H_{x-x}	24.0	18.0
	H_{y-y}	28.3	15.0
	Z	7.9	20.0
-25 m	H_{x-x}	20.6	18.0
	H_{y-y}	17.0	20.0
	Z	9.8	16.5
-50 m	H_{x-x}	11.4	23.0
	H_{y-y}	13.4	35.0
	Z	7.8	9.5

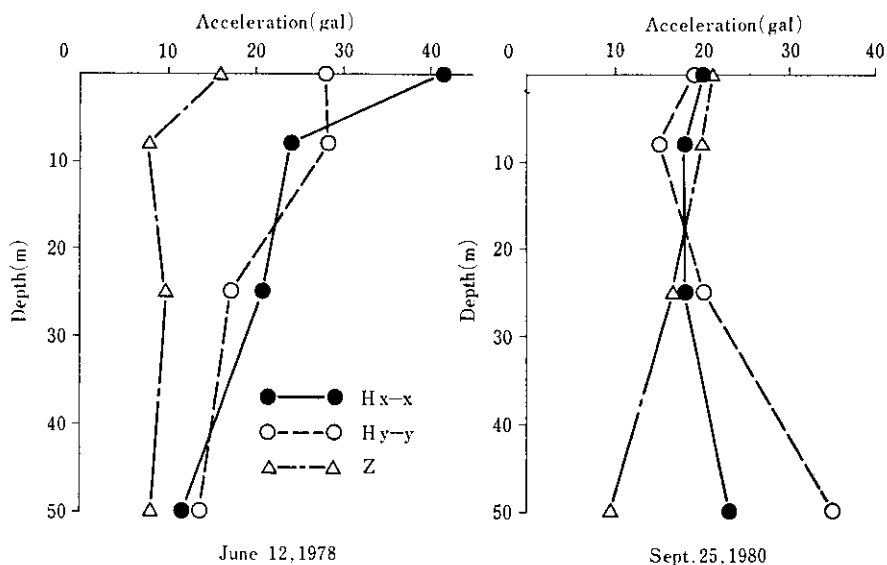


Fig. 6 Vertical distribution of maximum acceleration

ground acceleration shown in Fig. 6. In the case of long-distance type earthquakes¹⁾ observed up to the present, maximum acceleration in the horizontal direction of the ground decreases along with the ground depth; and that in the vertical direction of the ground tends to remain almost constant or slightly decrease along with the ground depth. On the contrary, in the case of "directly under" type earthquakes such as occurred recently, maximum acceleration in the horizontal direction of the ground tends to increase, except for the ground surface along with the ground depth. Whereas that in the vertical direction of the ground tends to decrease along with the ground depth. The seismic observation conducted this time is an exceptionally rare case with its very short epicentral distance and its small depth of hypocenter, as mentioned above. So much so that, examples of similar seismic observation are very few. Accordingly, the observation is not applicable to the evaluation of generality of the abovementioned phenomena. In view of the distribution recently reported by "directly under" type earthquakes which occurred in El Asnam of Algeria, Mexico, etc., these earthquakes clearly show

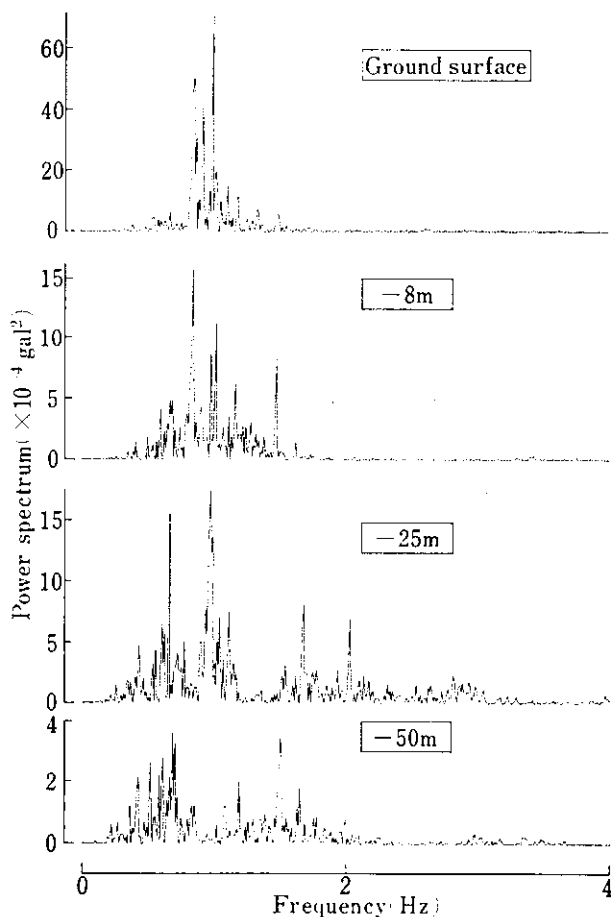


Fig. 7 Power spectrum (June 12, 1978)

that vertical acceleration should not be neglected in aseismic designs. In this respect, the present seismograms are considered to be valuable data.

4 Analysis of Observation Results

The play-back data of signals stored on the magnetic tape are sampled at 81.92 Hz and 40.96 Hz. After A/D conversion of the data ranging from the initially detected seismic wave to 50 sec. and to 100 sec., the power spectrum, correlation function and response spectrum were calculated using the Fourier analyzer.

4.1 Frequency Characteristic of Observation Records

The power spectrum of ground acceleration in the direction of the horizontal component (N-S) of the long-distance type earthquakes (June 12, 1978) and "directly under" type earthquakes (Sept. 25, 1980) are shown in Figs. 7 and 8. It is observed from Fig. 7 that waves of a fairly definite frequency range are present on the surface and down to -8 m, and the frequency of seismic wave spreads to a wide range at -25 m and -50 m. That is, waves of 0.84 to 0.98 Hz prevail on the ground surface and at -8 m, and spread to a frequency range of 0.41 to 1.98 Hz at -25 m and -50 m. This tendency bears a close resemblance to the spectrum characteristics of the past long-distance type medium- to small-scale earthquakes and long-period waves which are observed in the ground below -25 m

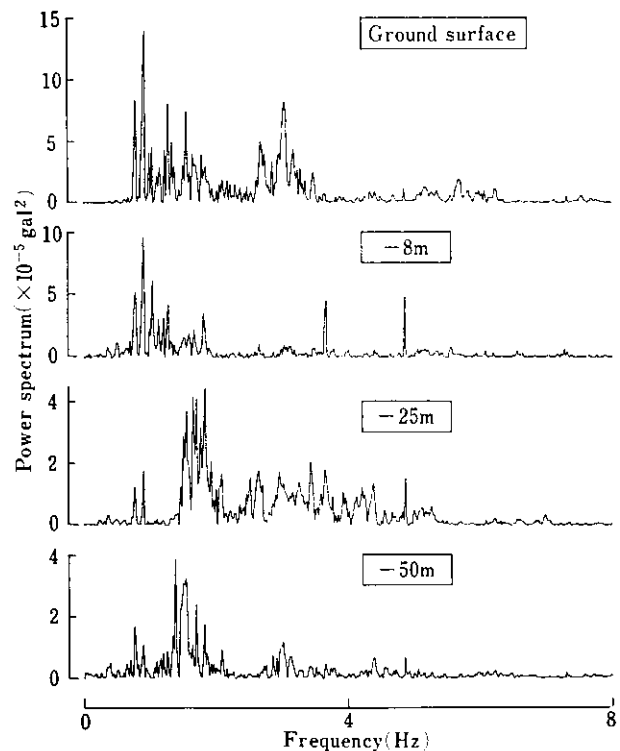


Fig. 8 Power spectrum (Sept. 25, 1980)

disappear on the surface and in the ground below -8 m. From these spectra and from the results of measurement by microtremors conducted separately, the predominant wave frequency of ground at this site is estimated at about 0.85 to 0.95 Hz.

On the other hand, in the case of the "directly-under" type earthquakes shown in Fig. 8, the power spectrum coincides with the known fact that the power spectrum extends to the high-frequency range when the hypocentral distance is very short. It is, however, noteworthy that it has the peak value at about 3 Hz on the ground surface. This is considered to be due to the influences of higher mode of the ground.

Nevertheless, at all the distances from the surface to -50 m in the present earthquakes, a peak value has occurred in the range of about 0.85 to 0.95 Hz. Therefore, the peak value is considered to be the aforementioned predominant wave frequency.

4.2 Wave Analysis of Observation Records

Wave analysis was performed by calculating the self-correlation function of horizontal component (N-S) of the observed acceleration records.

Fig. 9 shows the auto-correlation functions of long-distance type earthquakes. Although the wave motion is relatively predominant at -25 m, somewhat random wave motion is prevalent at -8 m, which is 17 m above the level of -25 m. That is, in this example, random waves are observed in the ground of -50 m,

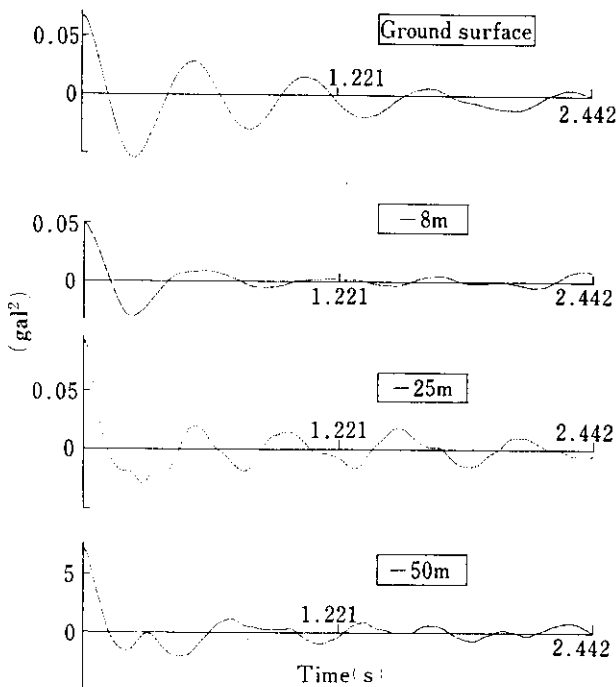


Fig. 9 Auto correlation functions (June 12, 1978)

become periodic at -25 m in the course of transmission through soft ground, and then become prevalent again at -8 m. Finally the random waves become periodic again on the surface.

On the other hand, in Fig. 10 which shows the auto-correlation function, the process of transmission of waves from -50 m to -8 m assumes a form which is relatively analogous to that of the aforementioned long-distance type earthquakes, but on the ground surface which is the last stage of transmission, the wave is not made periodical and the random waves are prevalent. This characteristic suggests that "directly under" type earthquakes are more susceptible to the influence of the higher mode of the ground than the long-distance type earthquakes.

Next, from the observation results at two points in the ground at different depths, the cross correlation function of the two was calculated and shown in Fig. 11. The values of v_s in the figure are obtained by dividing the distance between the two points by the time during which waves propagate over the same distance, by assuming that the delay time to the initial peak shown in the correlation diagram is the time during which waves propagate between the two points. Therefore, these v_s values may be taken as the average propagation velocity of the S wave between the two points, and thus it can be found that this ground is generally very soft. This is almost the same tendency with the S wave velocity obtained from the results of

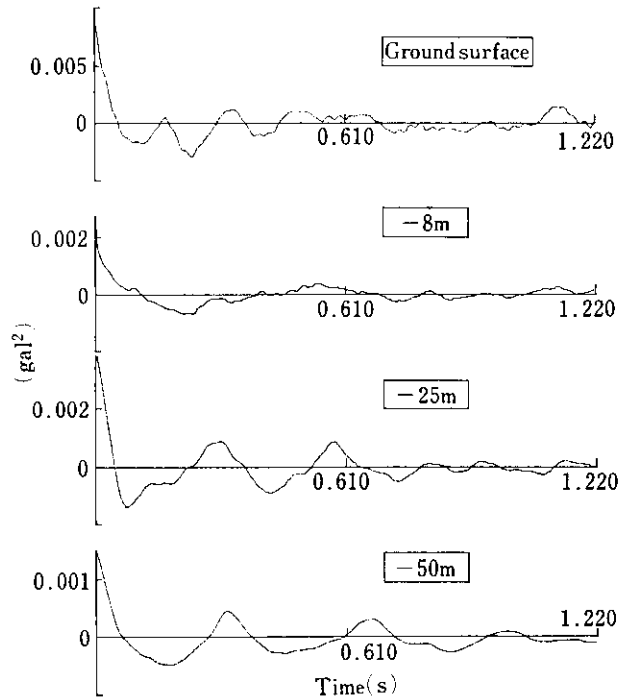


Fig. 10 Auto correlation functions (Sept. 25, 1980)

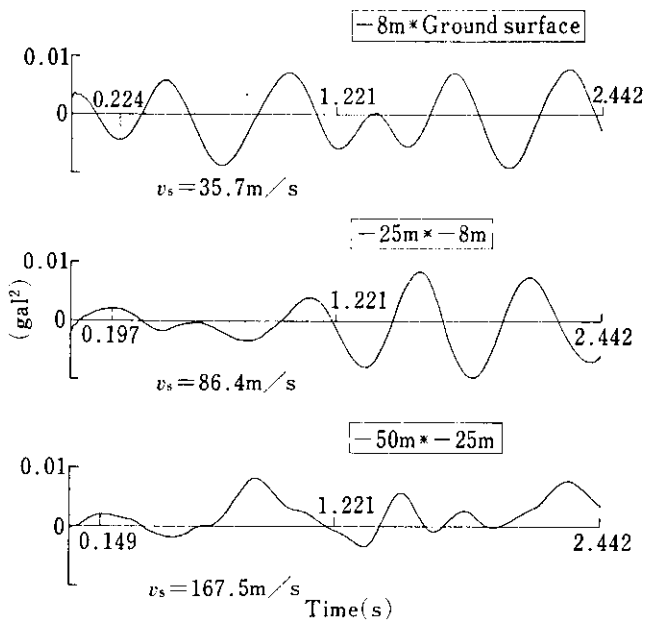


Fig. 11 Cross correlation functions (June 12, 1978)

the seismic prospect²⁾ when soil improvement work was executed.

4.3 Response Spectrum Based on Acceleration Records

In order to examine the characteristics of long-distance type earthquakes and "directly under" type earthquakes from the aspect of response by structures, the acceleration and velocity response spectra of the one degree of freedom system were obtained by the following equations using the horizontal component of ground surface acceleration (N-S) on the acceleration records obtained by observation:

$$S_a = \omega_d \left| \int_0^t \ddot{y}(\tau) e^{-h\omega_d(t-\tau)} \left\{ \left(1 - \frac{h^2}{1-h^2} \right) \times \sin \omega_d(t-\tau) + \frac{2h}{\sqrt{1-h^2}} \cos \omega_d(t-\tau) \right\} \times d\tau \right|_{\max} \dots\dots\dots(1)$$

$$S_v = \left| \int_0^t \dot{y}(\tau) e^{-h\omega_d(t-\tau)} \left\{ \cos \omega_d(t-\tau) - \frac{h}{\sqrt{1-h^2}} \sin \omega_d(t-\tau) \right\} d\tau \right|_{\max} \dots\dots\dots(2)$$

- S_a : Acceleration response spectrum
- S_v : Velocity response spectrum
- ω_d : Natural angular frequency of structure

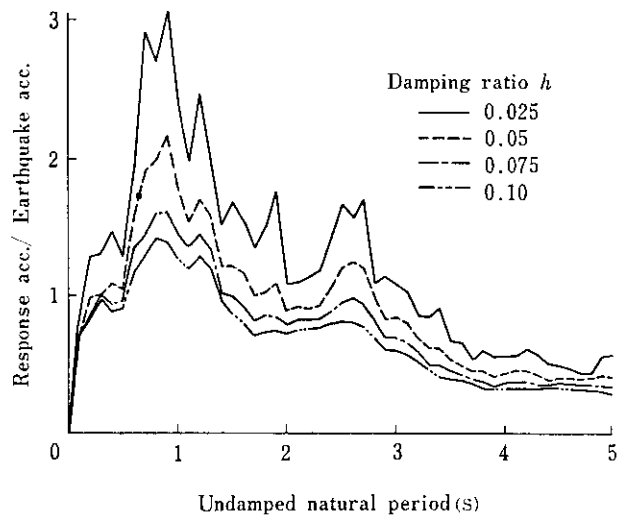


Fig. 12 Acceleration response spectra (June 12, 1978)

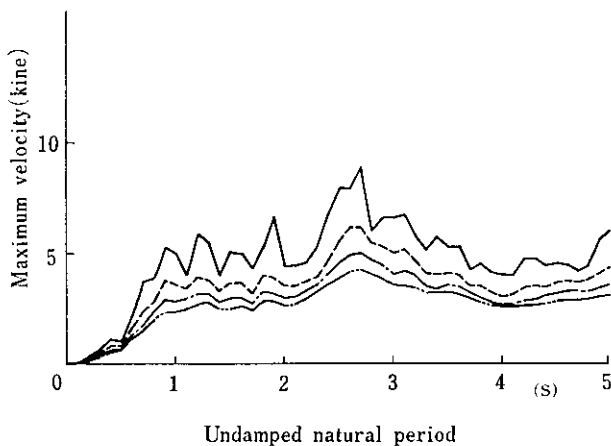


Fig. 13 Velocity response spectra (June 12, 1978)

- h : Damping constant
- \ddot{y} : Acceleration time history
- t : Time
- τ : Delay time

Figs. 12 and 13 show acceleration response spectra and velocity response spectra for long-distance type earthquakes respectively, and Figs. 14 and 15 show those for the "directly under" type. In these figures, the ordinate for the acceleration response spectrum shows non-dimensional quantity $S_a/\ddot{y}(\tau)$ obtained by dividing maximum response acceleration S_a generated in the one degree of freedom system by maximum acceleration $\ddot{y}(\tau)$ on the seismic record which was used as input, and the ordinate for the velocity response spectrum shows the maximum value of response velocity of the one degree of freedom system.

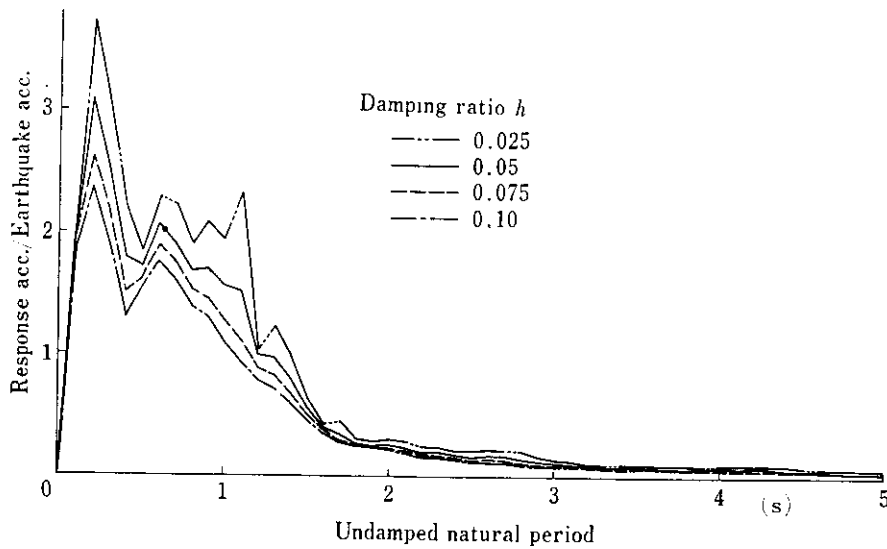


Fig. 14 Acceleration response spectra (Sept. 25, 1980)

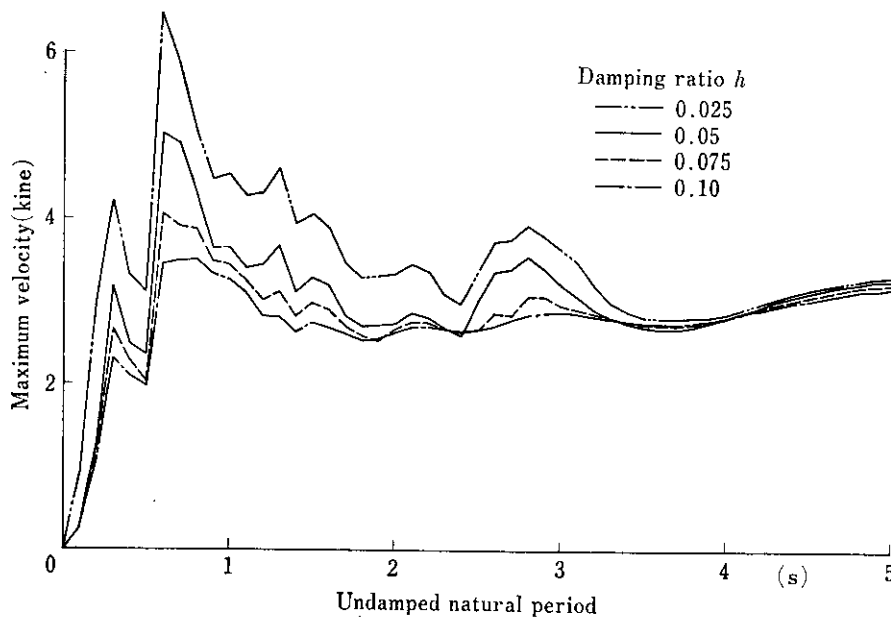


Fig. 15 Velocity response spectra (Sept. 25, 1980)

The abscissa shows the undamped natural period of the structure. The parameter is the damping ratio.

From the spectrum diagrams given in Figs. 12 and 14, the undamped natural periods that show respective peak values are 0.9 and 0.2 sec. Further, the former spectrum maintains a certain magnitude until the undamped natural period of the structure becomes about 3 sec., and is gradually damped over the longer period, whereas the spectrum of the latter is abruptly damped when the natural period becomes more than

1 sec. This suggests that long-distance type earthquakes are apt to exert a large influence on the structure of relatively longer period and "directly under" type tends to exert influence on the shorter period structure.

That is, in respect of the response of No. 6 blast furnace structure, this structure is more easily liable to resonate to long-distance type earthquakes than to the "directly under" type considering the fact that the natural period of the structure system inclusive of the

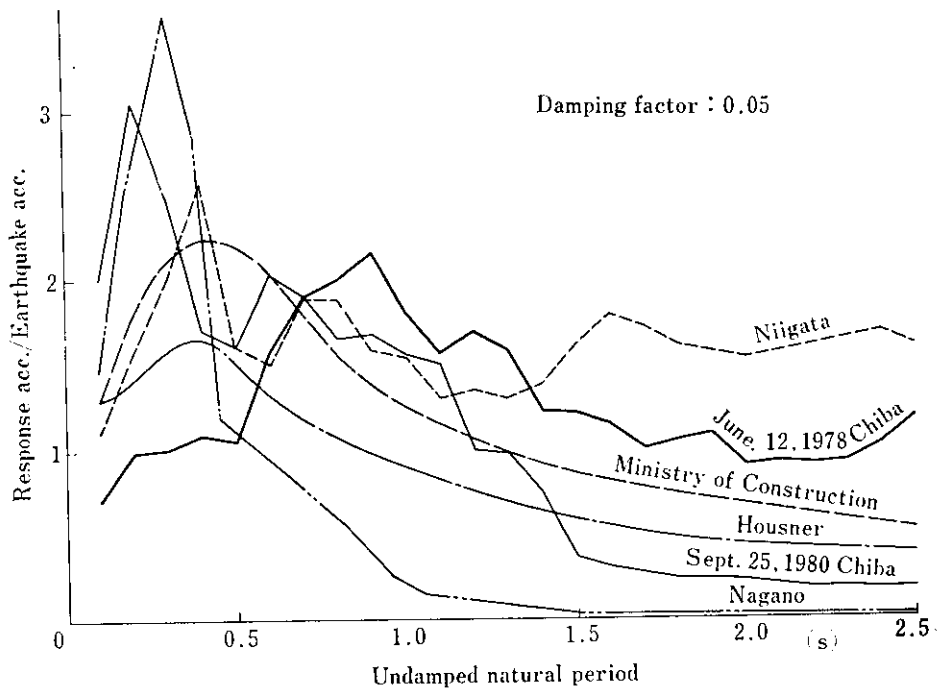


Fig. 16 Comparison of acceleration response spectra with past data

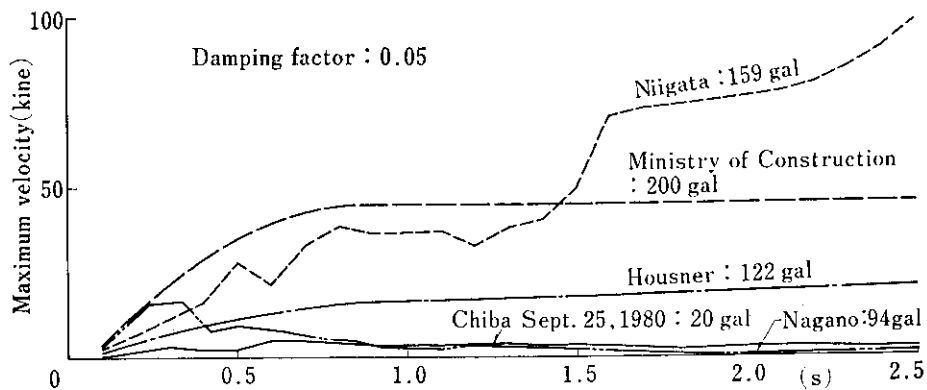


Fig. 17 Comparison of velocity response spectra with past data

upper structure and foundation of the blast furnace is 1.1 sec. However, these theories apply only to the horizontal component of input acceleration. Since the vertical component at the time of "directly under" type earthquakes is considered to greatly influence this structure as mentioned earlier, studies must also be made on the rotation moment due to the weight of the furnace and the position of gravity center of the furnace foundation.

The velocity response spectra given in Figs. 13 and 15 also show similar characteristics to the above-mentioned acceleration response spectra. In Fig. 13,

the structure of a relatively longer period is greatly affected, whereas in Fig. 15, the structure of a shorter period is greatly affected. However, the general tendency determined by the results of analyses of many past records of strong earthquake, indicating that the velocity response spectra show nearly fixed values when the natural period of structures is above 1 sec., still applies.

Figs. 16 and 17 compare such relations. Long-distance type earthquakes shown in Fig. 16 indicate a similar tendency to spectra provided by the Ministry of Construction of Japan and also by Housner. How-

ever, the natural period which shows its peak value becomes relatively longer. On the other hand, "directly under" type earthquakes show an analogous tendency to the results of observation at Nagano of the MATSUSHIRO region earthquakes suggesting the possibility of occurrence of maximum acceleration more than three times as large as ground motion acceleration in a shorter period structure having a natural period of about 0.2 sec. This also means that great influence is not exerted on the structure having a natural period of more than 1.5 sec. Such a small response of the structure having a relatively longer period can be attributable to the very short hypocentral distance and small depth of the hypocenter as well as the consequent abundance of waves of a relatively shorter period which prevent the response of the longerperiod structure from becoming larger.

The velocity response spectra shown in Fig. 17 naturally change in shape depending on the magnitude of input earthquake motion, but it is generally said that the velocity response spectra often show a more or less constant trend regarding the period, and the spectra of the "directly under" type earthquake (Sept. 25, 1980) also show the same tendency as with the Ministry of Construction, Housner and Nagano giving more or less constant values at a natural period above 0.75 sec.

5 Earthquake Resistance of No. 6 Blast Furnace Foundation

In constructing the foundation of the blast furnace which is the symbol of steelworks, a dynamic analysis was performed bearing in mind the response of the ground and placing stress in the comparative design of the foundation on its earthquake-proof structure, taking into account the fact that the ground of the construction site is soft and is in an earthquake-prone zone.

5.1 Dynamic Design

As shown in Fig. 18, the actual structure was transposed by a lumped mass model.^{3,4)} The upper structure consisted of a three-mass model of the bending and shearing type. The lower structure comprised a four-mass model of the bending and shearing type according to the shape of the foundation and nature of the ground. As the existing ground in the coupled vibration model, a four-mass model of the shearing type was used, and as the equivalent soil a four-mass model of the shearing type was used, assuming that the ground around the foundation is the equivalent soil. The damping constant was presumed as 10% for the structure and ground, taking into consideration the material damping and escape damping. The results

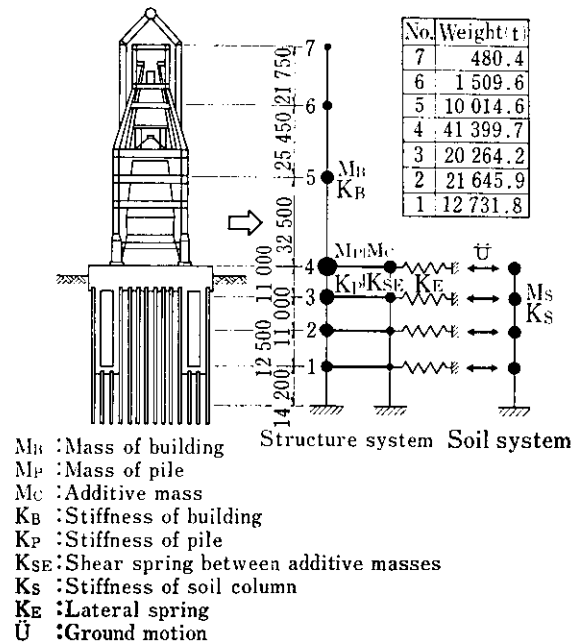


Fig. 18 Analytical model of soil-structure coupled system

obtained for the coupled vibration model are as follows: The maximum acceleration in the ground of input seismic waves in this case was assumed as 130 gal. Generally, this assumption of maximum acceleration is made from magnitude M and epicentral distance Δ ⁵⁾. If large-scale earthquakes of the long-distance type ($M = 8$, $\Delta = 100$ km) are supposed, presumed maximum acceleration generated in the ground is 110 gal, and in the case of medium-scale, short-distance earthquakes ($M = 7$, $\Delta = 30$ km), maximum acceleration is about 130 gal. Therefore, calculation was made in the coupled vibration model analysis on the assumption that maximum input acceleration is 130 gal. Three earthquakes i.e., EL CENTRO earthquake which is often used for a response analysis as representative earthquake, Chiba earthquake (Nov. 16, 1974) and Chiba earthquake (Feb. 8, 1975) are used for seismic waveforms. From the modal analysis, the natural period was found to be 0.847 sec. for the model in which the upper structure, foundation, equivalent soil and horizontal spring were taken into consideration. Fig. 19 illustrates the story-shearing coefficient. From the figure it is seen that the greatest story-shearing coefficient is for Chiba (Nov. 16, 1974) and the smallest is for Chiba (Feb. 8, 1875). This indicates that response acceleration for the coupled vibration model depends largely on the predominant period, since the predominant periods of the response spectra for seismic waves of various areas are; 0.6 to 0.7 sec. in EL CENTRO, about 0.7 sec. in

Chiba (Nov. 16, 1974) and about 0.2 sec. in Chiba (Feb. 8, 1974). Further, the displacement of the upper structure (7 mass) was 4.5 to 12.7 cm, and that at the upper end of the well foundation composed of steel pipe piles was 1.0 to 2.1 cm. Especially, the response value of the foundation part was very small. This may be attributable to the fact that the rigidity of the foundation was enhanced by adopting the double wall typed well foundation composed of steel pipe piles, instead of conventional well foundation, and by excavating between outer walls to deposit concrete, and that the ground was compacted by the second improvement work.

Fig. 19 also shows the story-shearing coefficient obtained from the design seismic coefficient used for static designing of the structure. The result of coupled vibration analysis was obtained on the assumption that the structure was linear. However, the structure has considerable proof stress after yielding, and as a method to evaluate the proof stress, the way to allow upto 3 to 5 times the deformation at the time of yielding is used. If the structure is supposed to be an elasto-plastic body, and the proof stress after yielding is evaluated to be allowable upto three times the deformation at the time of yielding, $P_0 = \sqrt{5}P$ will result

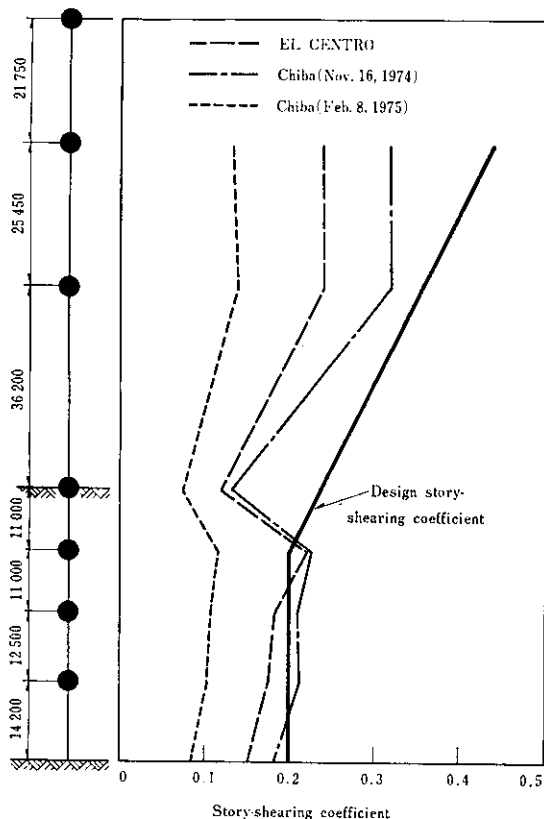


Fig. 19 Story-shearing coefficient calculated from analytical model

from the equilibrium of energy⁶⁾, and it follows that proof stress of the structure P_0 is 2.236 times as large as yielding load P . In consideration of this point, the story-shearing coefficient was calculated as shown in Fig. 19, by dividing the horizontal force acting on the upper structure—out of the results of the analysis by the coupled vibration model—by 2.236.

The story-shearing coefficient obtained by the coupled vibration analysis in Fig. 19 is smaller than the design shear coefficient both in the upper structure and foundation. Especially, the design seismic intensity 0.2 used for designing of the foundation can be said to be an adequate value.

Table 3 Maximum acceleration of No. 6 blast furnace at the points shown in Fig. 1 against observed earthquakes

Location	Response maximum acceleration (Gal)		
	June 12, 1978	Sept. 24, 1980	Sept. 25, 1980
P1 X-X	38.8	27.8	114.5*
P1 Y-Y	45.0	30.0	123.6*
P1 Z-Z	8.5	13.0	30.0
P2 X-X	149.9*	64.4	265.3*
P2 Y-Y	96.3*	58.0	238.9*
P2 Z-Z	22.5	19.4	79.9
P3 X-X	135.9*	40.0	92.5
P3 Y-Y	72.8*	30.6	126.1*
P3 Z-Z	15.3	10.0	46.3
P4 X-X	142.9*	—	—
P4 Y-Y	45.0	22.8	94.0
P4 Z-Z	11.0	8.5	47.5
P5 X-X	21.5	10.0	26.3
P5 Y-Y	19.0	7.8	30.6
P5 Z-Z	9.3	6.0	14.8
P9 X-X	15.0	—	—
P9 Y-Y	14.5	6.7	27.6*
P9 Z-Z	7.6	7.0	13.0
P13 X-X	10.2	—	—
P13 Y-Y	10.2	12.0	49.4*
P13 Z-Z	9.2	5.9	18.0
P11 X-X	9.0	10.0	41.2*
P11 Y-Y	8.8	8.0	33.0*
P11 Z-Z	6.4	6.0	17.2
P15 X-X	7.8	8.0	18.5
P15 Y-Y	6.8	5.5	19.0
P15 Z-Z	4.1	3.0	10.8

* Estimated values

5.2 Results of the Actual Earthquake Observation

Since the above-mentioned dynamic design is only a model analysis, the best way to verify its adequacy is to investigate the response characteristics of actual structures by actual earthquake motion. Here, discussion will be made by selecting two types of earthquakes, i.e., the "directly under" type and long-distance type, described in Chapter 3, which showed the greatest response since the commencement of actual earthquake observation.

The earthquake acceleration of No. 6 BF is shown in Table 3 and the distribution of story-shearing coefficients, converted from Table 3, is given in Fig. 20. The story-shearing coefficient of "directly under" type earthquake which occurred on September 24 is also indicated in the figure.

What can be commonly said about Fig. 20 is that the story-shearing coefficient of the upper structure increases more rapidly than that of lower structure. This tendency accords with the results of past medium- to small-scale earthquakes, and the greater the input acceleration of the ground, the greater the rate of increase. When the story-shearing coefficient of 0.24 of

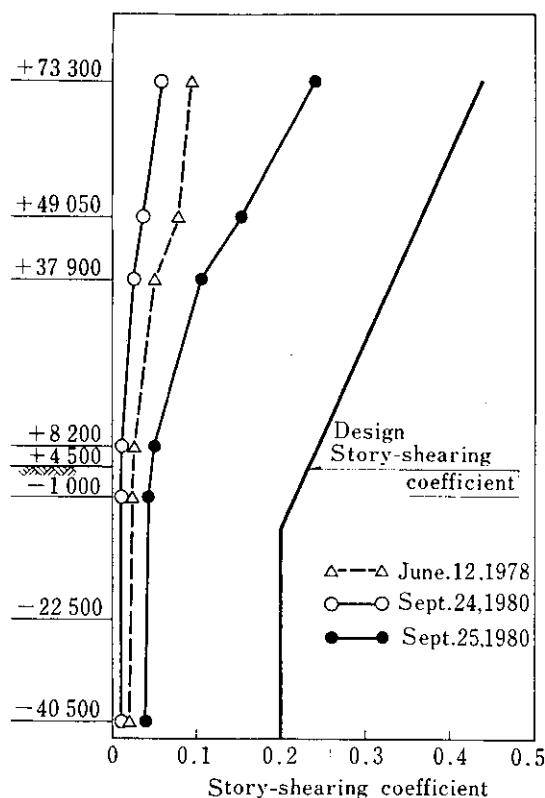


Fig. 20 Story-shearing coefficient calculated from maximum response acceleration shown in Table 3

the uppermost layer at the time of the Sept. 25 earthquake—which showed the greatest response acceleration out of the above-mentioned major-intensity earthquakes—is compared with the design story-shearing coefficient of 0.45, it is found that the former is a little less than half of the latter. Therefore, some damage to the structure is anticipated, if it is struck by an earthquake twice as large as the Sept. 25 earthquake.

6 Conclusions

From a series of seismic observation conducted at No. 6 BF of Chiba Works and surrounding soft ground with emphasis placed on actual experience of "directly under" type earthquakes of the largest magnitude class, the dynamic deformation characteristics of the soft ground layer were grasped, and specific characteristics of an important structure such as the blast furnace, viewed from the point of aseismic engineering, were clarified, with some knowledge on aseismic designs obtained. The results obtained are summarized as follows:

- (1) In the long-distance type earthquakes, maximum acceleration in the horizontal direction of the ground decreases along with the ground depth; and that in the vertical direction of the ground tends to remain almost constant or slightly decrease along with the ground depth. Whereas, in the "directly under" type earthquakes, maximum acceleration in the horizontal direction of the ground tends to increase, except on the ground surface, along with the ground depth; and that in the vertical direction of the ground tends to decrease along with the ground depth, both influenced by the surface waves.
- (2) The frequency analysis of observed seismic waves shows that the predominating frequency of the ground is about 0.9 Hz. The range of frequency is relatively narrow for "long-distance" type earthquakes, and spreads widely for the "directly under" type.
- (3) The average propagation velocity of *S* waves obtained from the cross correlation function of seismic waves shows a reasonable value.
- (4) When the natural period of the structure system including the superstructure of the blast furnace and its foundation is considered from the response spectra, it can be said that this structure is more liable to resonate with long-distance type earthquakes than with the "directly under" type, and it is considered that the vertical component of "directly under" type earthquakes exerts a large influence on this structure. Therefore, it is urgently necessary to conduct research on this aspect.

- (5) The story-shearing coefficient converted from the response spectrum showed nearly the same value as the design story-shearing coefficient for the foundation structure. For the superstructure, however, the value shown is on the risky side, when inferred from the story-shearing coefficient obtained from the actually measured value.
- (6) Should ground acceleration a little less than 11 times that of the largest-scale long-distance type earthquake (June 12, 1978) or a little less than 2 times that of the largest-scale "directly under" type earthquake (Sept. 25, 1980) ever recorded since the start of observation, it would exceed the design shearing coefficient for the uppermost layer.

References

- 1) T. Yamasaki and M. Ishida: "Observation and Analysis of Earthquake Motion on Soft Ground," 6th Southeast Asian Conference on Soil Engineering, Taipei, (1980)
- 2) K. Tsutsumi, M. Nei and I. Jo: "Improvement Work for Weak Ground at Chiba West Site", *Kawasaki Steel Technical Report*, **10** (1978) 2-3, pp. 5-18 (in Japanese)
- 3) N. Tominaga, Y. Echigo, H. Uchiyama and M. Hashimoto: "A Newly Developed Realtime Construction Control System in Civil Engineering Works: Part I", *Kawasaki Steel Technical Report*, **9** (1977) 3-4, pp. 81-95 (in Japanese)
- 4) T. Yamasaki, M. Tominaga, H. Yukitomo and M. Ishida: "Lateral Resistance of Pipe Pile Well Foundation", X ICSMFE, Stockholm, (1981) (Manuscript submitted)
- 5) S. Okamoto: *Aseismic Engineering* (1971), p. 110 (Ohmsha)
- 6) K. Muto: *Aseismic Design Series 1—Aseismic Calculation*, (1963), pp. 16-17 (Maruzen)